

# Adaptive Nonlinear Model Reduction for Fast Power System Simulation

Denis Osipov, *Student Member, IEEE*, and Kai Sun, *Senior Member, IEEE*

**Abstract**--The paper proposes a new adaptive approach to power system model reduction for fast and accurate time-domain simulation. This new approach is a compromise between linear model reduction for faster simulation and nonlinear model reduction for better accuracy. During the simulation period, the approach adaptively switches among detailed and linearly or nonlinearly reduced models based on variations of the system state: it employs unreduced models for the fault-on period, uses weighted column norms of the admittance matrix to decide which functions to be linearized in power system differential-algebraic equations for large changes of the state, and adopts a linearly reduced model for small changes of the state. Two versions of the adaptive model reduction approach are introduced. The first version uses traditional power system partitioning where the model reduction is applied to a defined large external area in a power system and the other area defined as the study area keeps full detailed models. The second version applies the adaptive model reduction to the whole system. The paper also conducts comprehensive case studies comparing simulation results using the proposed adaptively reduced models with the linearly reduced model and coherency-based reduced model on the Northeast Power Coordinating Council 140-bus 48-machine system.

**Index Terms**--Linear model reduction, nonlinear model reduction, power system partitioning, power system simulation.

## I. INTRODUCTION

POWER system simulation is very important for grid operations and planning at electricity utilities. It can assess dynamic security under a certain operating condition of the studied power system following a given contingency such as loss of a transmission line or generator unit. Essentially, power system simulation is to obtain a time-series trajectory of the system state for a specified simulation window by solving the initial value problem of a set of nonlinear differential-algebraic equations co-determined by the mathematical model of the whole system, the operating condition and the contingency. Nowadays, the fast growth in electricity demand and a relatively slow construction of new transmission infrastructure are pushing power transmission systems to be operated closer to their stability limits and motivating the transition of power system simulation from the offline

planning stage to the real-time operation environment.

One way to increase the speed of simulation of a complex power grid is to conduct network partitioning and then model reduction. For example, a traditional approach defines a study area, which is an important small part of the system for dynamic security assessment, considering all the details, and reduces the model of the rest of the system, i.e. the external area. In practice, an additional buffer zone is often defined in between with moderate reduction to connect the study and the external areas [1]. The methods for model reduction on the external area can be divided into two main groups: the ones that preserve the structure of a power system and the ones that use mathematical transformations from original states to nonphysical states that are subsequently reduced.

The most widely used methods from the first group are coherency-based methods [2]-[4], which were originally developed for power system model reduction and conduct the following steps: coherency identification, aggregation of coherent generators, and network reduction. After the first step, the generators that oscillate together following a disturbance are included into one group. The groups of coherent generators are then aggregated into individual equivalent generators connected with each other by equivalent branches and with the study area by a reduced system network. This creates a unique boundary between the external area and the study area and does not allow arbitrary division between areas. In addition, if the topology of the original system changes, it can affect the coherency and consequently the split between the study area and the generator grouping of the external area. This can change the boundary in between. Thus, the grouping of generators based on coherency has an inherent limitation on the way a system can be partitioned.

The second group of methods does not have that limitation as the states are transformed into a new state space. Thus, the system can be partitioned in any way. These methods came from the control field of engineering. In the most used methods from this category, the external area model is first linearized and then reduced using balanced truncation [5]-[7] or Krylov subspace methods [8]-[10]. The linearization of the model gives acceptably accurate results when concerned disturbances are small but once the size of the disturbance increases the linearized model cannot guarantee an accurate representation of the original part of the system. To improve the accuracy of large-disturbance simulation, nonlinear model reduction methods can be used. References [11]-[12] propose using empirical controllability and observability covariance matrices that contain nonlinear behavior of the system around

---

This work was supported in part by the ERC Program of the NSF and DOE under NSF grant EEC-1041877 and in part by the NSF grant ECCS-1610025.

D. Osipov and K. Sun are with the Department of Electrical Engineering and Computer Science, University of Tennessee, Knoxville, TN 37996 USA (email: dosipov@vols.utk.edu, kaisun@utk.edu).

the operating condition. In [13]-[14] the authors try to generalize and extend the linear balance truncation to nonlinear systems. A proper orthogonal decomposition method is described in [15], whose error and computational complexity are analyzed. As shown in [15]-[16], application of nonlinear model reduction cannot give substantial computational time decrease as compared to the original model. In addition, some methods require training simulation data to create a reduced model, which cannot guarantee adequate performance during all possible disturbances. If a disturbance is very different from that with the training set, the model reduction error can substantially increase [17].

Compared to the existing work this paper proposes a new adaptive model reduction approach, which is a compromise between linear model reduction and nonlinear model reduction in terms of accuracy and speed of time-domain simulation using the reduced model. A comprehensive study is also presented to compare this adaptive model reduction approach with the linear model reduction approach and the coherency-based model reduction approach. During the simulation period, the approach adaptively switches among detailed and linearly or nonlinearly reduced models based on variations of the system state: it employs unreduced models for the fault-on period, uses weighted column norms of the admittance matrix to decide which functions to be linearized in the power system model for large changes of the state, and adopts a linearly reduced model for small changes of the state.

The version of the adaptive approach described above uses traditional topological power system partitioning with the study area and the external area. This partitioning creates an additional error that can affect the performance of the model reduction. To address the partitioning error the second version of the adaptive approach is proposed where the model reduction is performed to the whole system.

Thus, the main contributions of this paper are in these three aspects: 1) a new model reduction approach is proposed that enables adaptive switches among the detailed model, the linear reduced model and the hybrid reduced model having only certain functions linearized; 2) unlike most of existing model reduction methods that need to partition the whole power network into a study area with detailed models and external area with reduced models, the new approach can be applied to either a partitioned external area only or the whole system without network partitioning; 3) the proposed approach with and without partitioning is compared with the traditional coherency-based and linear model reduction methods by comprehensive case studies on realistic power system models.

The remainder of this paper is organized as follows. Section II describes the model and the approach used in power system partitioning, presents the linear model reduction approach and proposes the adaptive model reduction approach including the model reduction method as a hybrid of nonlinear and linear model reduction techniques, the algorithm enabling adaptive switching among models of different levels of details and the second version of the adaptive approach that can be applied to the whole power system. In Section III the proposed approaches are tested together with the traditional linear and

coherency-based model reduction approaches on the Northeast Power Coordinating Council (NPCC) 48-machine 140-bus system. Finally, conclusions are drawn in Section IV.

## II. PROPOSED ADAPTIVE MODEL REDUCTION

### A. Power System Partitioning

As it was mentioned above, in power system model reduction the system is divided into two areas: 1) the study area, which is the main interest of an investigator, where all details are preserved, and all disturbances are originated from; 2) the external area, which can be simplified and reduced. The partitioned power system is shown in Fig. 1.

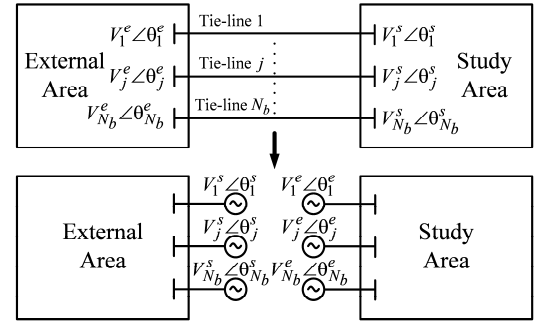


Fig. 1. Power system partitioning.

The study area of the original system is connected to the external area by several tie-lines. For the study area, a tie-line  $j$  is treated as a simple fictitious generator with the internal voltage phasor equal to a voltage phasor  $V_j^e \angle \theta_j^e$  of the corresponding boundary bus in the external area and with the armature resistance and transient reactance equal to the resistance and reactance of a tie-line  $j$ . Likewise for the external area, a tie-line  $j$  is treated as a generator with the internal voltage phasor equal to a voltage phasor  $V_j^s \angle \theta_j^s$  of the corresponding boundary bus in the study area. During each iteration of the system simulation these fictitious generators are treated as constant voltage sources and represent the current injections from one area to the other area. Therefore, voltage magnitudes and voltage angles of boundary buses in one area are the inputs to the model of the other area. At every iteration, each area is calculated separately, then the boundary bus voltage phasors of both areas are recalculated, and their values are sent as inputs to the corresponding area to perform the next iteration. As constant voltage sources the fictitious generators do not have inertias or contribute to the dynamics of each area as a component of the differential equations of generators inside the corresponding area.

In this paper, each generator is represented by a detailed two-axis model with a non-reheat steam turbine model, a first-order governor model and an IEEE type 1 exciter model [18], as described these nine differential equations:

$$\begin{cases}
\dot{\delta}_i = \omega_{base} (\omega_i - 1) \\
T_{chi} \dot{P}_{m_i} = -P_{m_i} + P_{gvi} \\
T_{gvi} \dot{P}_{gvi} = -P_{gvi} + P_{ref_i} - \frac{(\omega_i - 1)}{R_i} \\
T_{A_i} \dot{V}_{R_i} = -V_{R_i} + K_{A_i} R_{f_i} - \frac{K_{A_i} K_{F_i}}{T_{F_i}} E_{fd_i} + K_{A_i} (V_{ref_i} - V_{t_i}) \\
T_{F_i} \dot{R}_{f_i} = -R_{f_i} + \frac{K_{F_i}}{T_{F_i}} E_{fd_i} \\
T_{E_i} \dot{E}_{fd_i} = -\left( K_{E_i} + A_{E_i} e^{B_{E_i} E_{fd_i}} \right) E_{fd_i} + V_{R_i} \\
T'_{qoi} \dot{E}'_{d_i} = -E'_{d_i} + (X_{q_i} - X'_{q_i}) I_{q_i} \\
T'_{do_i} \dot{E}'_{q_i} = -E'_{q_i} - (X_{d_i} - X'_{d_i}) I_{d_i} + E_{fd_i} \\
2H_i \dot{\omega}_i = P_{m_i} - E'_{d_i} I_{d_i} - E'_{q_i} I_{q_i} - D_i (\omega_i - 1)
\end{cases} \quad (1)$$

where

$$\begin{aligned}
I_{d_i} &= \sum_{j=1}^{N_g} E'_{d_j} (G_{ij} \cos \delta_{ij} + B_{ij} \sin \delta_{ij}) + \sum_{j=1}^{N_b} E'_{q_j} (G_{ij} \cos \delta_{ij} - B_{ij} \sin \delta_{ij}) \\
&\quad + \sum_{j=1}^{N_b} V_j \left[ G_{ij} \sin(\delta_i - \theta_j) - B_{ij} \cos(\delta_i - \theta_j) \right], \\
I_{q_i} &= \sum_{j=1}^{N_g} E'_{d_j} (-G_{ij} \cos \delta_{ij} + B_{ij} \sin \delta_{ij}) + \sum_{j=1}^{N_g} E'_{q_j} (G_{ij} \cos \delta_{ij} + B_{ij} \sin \delta_{ij}) \\
&\quad + \sum_{j=1}^{N_b} V_j \left[ G_{ij} \cos(\delta_i - \theta_j) + B_{ij} \sin(\delta_i - \theta_j) \right]
\end{aligned}$$

Here,  $\delta_i$  and  $\omega_i$  are the rotor angle and speed of generator  $i$  in rad and rad/s, respectively and  $\delta_{ij} = \delta_i - \delta_j$ ;  $\omega_{base} = 120\pi$  rad/s;  $P_m$ ,  $P_{gvi}$  and  $P_{ref_i}$  are the mechanical power, governor output and reference power, respectively;  $R_i$  is the speed regulation factor;  $E'_{d_i}$ ,  $E'_{q_i}$ ,  $X_{d_i}$ ,  $X_{q_i}$ ,  $X'_{d_i}$ ,  $X'_{q_i}$ ,  $I_{d_i}$  and  $I_{q_i}$  are the  $d$ - and  $q$ -axis internal voltages, synchronous reactances, transient reactances and currents, respectively, all in p.u.;  $V_{R_i}$ ,  $K_{A_i}$ ,  $R_{f_i}$ ,  $K_{F_i}$ ,  $E_{fd_i}$ ,  $V_{ref_i}$ ,  $V_{t_i}$ ,  $K_{E_i}$ ,  $A_{E_i}$  and  $B_{E_i}$  are the voltage regulator input, amplifier gain, rate feedback, feedback gain, field voltage, reference voltage, terminal bus voltage, exciter gain and exciter saturation coefficients;  $H_i$ ,  $T_{chi}$ ,  $T_{gvi}$ ,  $T_{A_i}$ ,  $T_{F_i}$ ,  $T_{E_i}$ ,  $T'_{qoi}$  and  $T'_{do_i}$  are respectively the generator inertia, turbine charging time, governor time constant, amplifier time constant, feedback time constant, the exciter time constant, the  $q$ -axis open circuit time constant and the  $d$ -axis open circuit time constant all in s;  $D_i$  is the damping coefficient;  $N_g$  and  $N_b$  are respectively the numbers of generators and boundary buses;  $G_{ij}$  and  $B_{ij}$  are conductance and susceptance between generator  $i$  and generator  $j$  in p.u.;  $V_j$  in p.u. and  $\theta_j$  in rad are respectively is the voltage magnitude and angle at boundary bus  $j$  in the opposite area.

### B. Model Reduction

If model reduction is applied to the external area it is

necessary to define state variables and inputs of the system. Considering that every generator is described by nine differential equations and every boundary bus has the voltage magnitude and angle as its parameters, let  $n = 9N_g$  and  $m = 2N_b$  respectively denote the numbers of state variables and inputs of the external area and let the outputs of the system be the state variables of the system. Then the system (1) can be described as the nonlinear system:

$$\begin{cases}
\dot{\mathbf{x}} = \mathbf{f}(\mathbf{x}, \mathbf{u}) \\
\mathbf{y} = \mathbf{x}
\end{cases} \quad (2)$$

where  $\mathbf{x} = (\delta \quad \mathbf{P}_m \quad \mathbf{P}_{gv} \quad \mathbf{V}_R \quad \mathbf{R}_f \quad \mathbf{E}_{fd} \quad \mathbf{E}'_d \quad \mathbf{E}'_q \quad \boldsymbol{\omega})^T$ ;  
 $\mathbf{u} = (\mathbf{0} \quad \mathbf{V})^T$ ;  $\mathbf{x} \in \mathbb{R}^n$  is the state vector;  $\mathbf{u} \in \mathbb{R}^m$  is the input vector;  $\mathbf{y} \in \mathbb{R}^n$  is the output vector.

#### 1) Linear Model Reduction:

Linearize system (2) around an equilibrium point as:

$$\begin{cases}
\Delta \dot{\mathbf{x}} = \mathbf{A} \Delta \mathbf{x} + \mathbf{B} \Delta \mathbf{u} \\
\Delta \mathbf{y} = \mathbf{C} \Delta \mathbf{x}
\end{cases} \quad (3)$$

where  $\Delta \mathbf{x}$ ,  $\Delta \mathbf{u}$  and  $\Delta \mathbf{y}$  are the deviation variables of respectively the original states, inputs and outputs;  $\mathbf{A} \in \mathbb{R}^{n \times n}$  is the matrix of partial derivatives of the functions in (1) with respect to each state evaluated at the equilibrium point;  $\mathbf{B} \in \mathbb{R}^{n \times m}$  is the matrix of partial derivatives of the functions in (1) with respect to each input evaluated at the equilibrium point;  $\mathbf{C} \in \mathbb{R}^{n \times n}$  is the identity matrix.

The system (3) can be reduced by a linear reduction method, e.g. the balanced truncation method [5], where transformation matrix  $\mathbf{T}$  and its inverse  $\tilde{\mathbf{T}}$  are calculated. Matrix  $\mathbf{T}$  transforms the state variables from the original state space to a new balanced state space:  $\Delta \tilde{\mathbf{x}} = \mathbf{T} \Delta \mathbf{x}$ .

In the resulted new balanced system, the state variables are arranged in a such way that the first one is the most controllable and most observable and the last is the least controllable and least observable. Henkel singular values show this relationship:  $\sigma_1 > \sigma_2 > \dots > \sigma_i > \dots > \sigma_{n-1} > \sigma_n \geq 0$ .

Because of the aforementioned fact that only first  $r$  state variables are kept, and the rest are truncated,  $H_\infty$  norm of the error of balanced truncation is bounded and satisfies:

$$\|\varepsilon\|_\infty \leq 2 \sum_{i=r+1}^n \sigma_i. \quad (4)$$

Recalculate the transformation matrix and its inverse as

$$\mathbf{T} = \mathbf{P} \mathbf{T}, \quad \tilde{\mathbf{T}} = \tilde{\mathbf{T}} \mathbf{P}^T, \quad (5)$$

where  $\mathbf{P} = (\mathbf{I} \quad \mathbf{0})$  is the identity matrix, the last  $(n-r)$  rows of which are deleted. Thus, the balanced truncated system is represented as (6), where  $\tilde{\mathbf{A}} = \mathbf{T} \mathbf{A} \tilde{\mathbf{T}}$ ;  $\tilde{\mathbf{A}} \in \mathbb{R}^{r \times r}$ ;  $\tilde{\mathbf{B}} = \mathbf{T} \mathbf{B}$ ;  $\tilde{\mathbf{B}} \in \mathbb{R}^{r \times m}$ ;  $\tilde{\mathbf{C}} = \mathbf{C} \tilde{\mathbf{T}}$ ;  $\tilde{\mathbf{C}} \in \mathbb{R}^{n \times r}$ .

$$\begin{cases} \Delta \dot{\tilde{\mathbf{x}}} = \tilde{\mathbf{A}}\Delta\tilde{\mathbf{x}} + \tilde{\mathbf{B}}\Delta\mathbf{u} \\ \Delta\mathbf{y} = \tilde{\mathbf{C}}\Delta\tilde{\mathbf{x}} \end{cases} \quad (6)$$

## 2) Proposed Hybrid Model Reduction:

In this paper, a model reduction method is proposed as a hybrid of nonlinear and linear model reduction techniques. As shown in [19]-[20], the transformation matrices  $\mathbf{T}$  and  $\tilde{\mathbf{T}}$  can be used to reduce the nonlinear system as well. In this case, the system can be represented as follows:

$$\begin{cases} \dot{\tilde{\mathbf{x}}} = \mathbf{T}\mathbf{f}(\tilde{\mathbf{T}}\tilde{\mathbf{x}}, \mathbf{u}) \\ \mathbf{y} = \tilde{\mathbf{T}}\tilde{\mathbf{x}} \end{cases} \quad (7)$$

The system in (7) has fewer states than the original system but it is still necessary to compute all nonlinear functions in  $\mathbf{f}$ . Thus, there is basically no reduction in computation time. To address that problem, ref. [21] suggests eliminating some of the functions. However, as it is shown in [22] it can create large errors due to the model reduction.

In the proposed hybrid model reduction approach, the functions that have the least contributions to the dynamics between the external area and a study area are not eliminated but linearized. To evaluate contributions of the functions, let us consider the expressions for the d-axis current and the q-axis current of generators in the external area as these expressions have most nonlinearities and are used in 33% of all differential equations in (1).

Nonlinearities in the expressions are cosine and sine functions and coefficients of these functions are conductances and susceptances between generators including fictitious generators representing the boundary between the external area and the study area. These values are real and imaginary parts of elements of the admittance matrix:  $Y_{ij} = G_{ij} + jB_{ij}$ .

The matrix can be divided into four submatrices:

$$\mathbf{Y} = \begin{pmatrix} \mathbf{Y}_{11} & \mathbf{Y}_{12} \\ \mathbf{Y}_{21} & \mathbf{Y}_{22} \end{pmatrix}, \quad (8)$$

where  $\mathbf{Y}_{11} \in \mathbb{R}^{N_g \times N_g}$  is the admittance matrix representing connections between generators inside the external area;  $\mathbf{Y}_{22} \in \mathbb{R}^{N_b \times N_b}$  is the admittance matrix representing connections between fictitious generators;  $\mathbf{Y}_{21} = \mathbf{Y}_{12}^T \in \mathbb{R}^{N_b \times N_g}$  is the admittance matrix representing connections between the generators of the external area and the fictitious generators.

Thus, column norms of absolute values of elements in matrix  $\mathbf{Y}_{21}$  can be used to determine which function to be linearized as the norms describe how close electrically each generator is to the boundary between the external area and a study area. Column norms are calculated by:

$$v_i = \sqrt{\sum_{j=1}^{N_b} |Y_{21ji}|^2}. \quad (9)$$

The nonlinear functions that correspond to the generators with large column norms are kept nonlinear and the nonlinear

generator functions with small column norms are linearized. Thus, the hybrid reduced system can be represented as

$$\begin{cases} \dot{\tilde{\mathbf{x}}} = \mathbf{T} \begin{pmatrix} \hat{\mathbf{f}}(\tilde{\mathbf{T}}\tilde{\mathbf{x}}, \mathbf{u}) \\ \mathbf{f}_l \end{pmatrix} \\ \mathbf{y} = \tilde{\mathbf{T}}\tilde{\mathbf{x}} \end{cases} \quad (10)$$

where  $\mathbf{f}_l = \hat{\mathbf{A}}\Delta\tilde{\mathbf{x}} + \hat{\mathbf{B}}\Delta\mathbf{u} + \hat{\mathbf{x}}^0$ ;  $\hat{\mathbf{x}}^0 = \hat{\mathbf{P}}\mathbf{x}^0$ ;  $\hat{\mathbf{A}} = \hat{\mathbf{P}}\mathbf{A}\tilde{\mathbf{T}}$ ;  $\hat{\mathbf{A}} \in \mathbb{R}^{(n-q) \times r}$ ;  $\hat{\mathbf{B}} = \hat{\mathbf{P}}\mathbf{B}$ ;  $\hat{\mathbf{B}} \in \mathbb{R}^{(n-q) \times m}$ ; Vector  $\hat{\mathbf{f}}$  comprises the functions that are kept nonlinear;  $\mathbf{f}_l$  has the linearized functions;  $\mathbf{x}^0$  is the initial state vector;  $\hat{\mathbf{P}}$  is the identity matrix with deleted rows that correspond to the functions in  $\hat{\mathbf{f}}$ ;  $q$  is the number of nonlinear functions in  $\hat{\mathbf{f}}$ .

## C. Adaptive Switching Algorithm

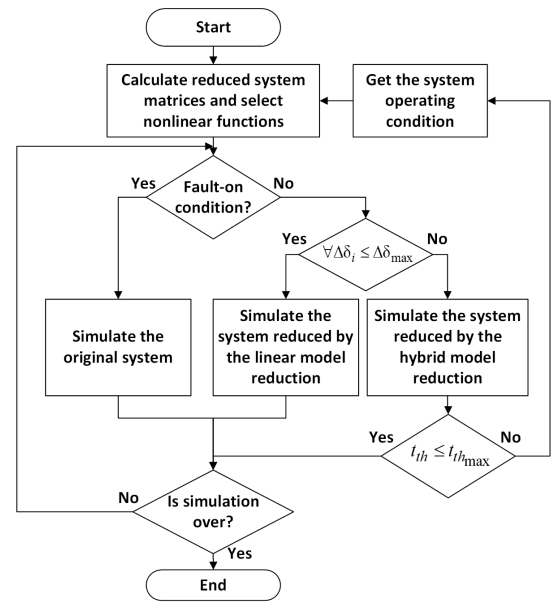


Fig. 2. Adaptive switching algorithm.

Considering that the linearly reduced system gives satisfactory performance during small disturbances, the duration of a large disturbance is short, and majority of the time a system is under small or no disturbance it is reasonable to change the type of the model reduction of the external system to increase the accuracy and speed of the system simulation. The proposed adaptive algorithm can adaptively change the complexity of the external area model based on the current condition as shown in Fig. 2.

During the fault-on period, the original, fully detailed system model is used as the maximum accuracy of the system model is required and the duration of a fault is limited to tens of milliseconds, which does not increase much the simulation time. To obtain the initial condition of the post-fault simulation the state vector from the last iteration of the fault-on simulation is multiplied by the transformation matrix. In the post-fault period, when the angle deviation  $\Delta\delta_i$  of any generator in a study area exceeds a preset threshold  $\Delta\delta_{\max}$ , the external area is reduced using the hybrid model reduction

method, which keeps the balance between accuracy and speed of simulation when the disturbance is large. In pre-fault and post-fault periods when all angle deviations are within the threshold, the external area is reduced using a linear model reduction method. This guarantees that most of the time when there is no disturbance or variation of the state is very small, the fastest model reduction method is applied.

To calculate the rotor angle deviation, the generator with the smallest column norm is used as a reference; i.e., the reference generator is the electrically farthest generator from a study area and has the least reactions to disturbances in study areas. If the time for a rotor angle deviation  $\Delta\delta_i$  exceeding threshold  $\Delta\delta_{\max}$ , denoted by  $t_{th}$ , is longer than a preset limit  $t_{th_{\max}}$  a new operating condition is obtained and matrices  $\tilde{\mathbf{A}}$  and  $\tilde{\mathbf{B}}$  of the linearly reduced system are recalculated. This action corrects the adaptive algorithm after a large change of the system state. As the linearization is performed offline and the update is only necessary when a substantial change of the operating condition occur, the matrix recalculation does not affect the speed of the algorithm over a long period of time. Thus, the proposed approach is scalable to deal with large power system models.

#### D. Adaptive Model Reduction without System Partitioning

Partitioning the system into the study area and the external area creates a specific error. The error is caused by the fact that the inputs (boundary bus voltage magnitudes and boundary bus voltage angles) are calculated at the previous iteration of the simulation, i.e. the inputs are lagging by one iteration. To eliminate the partitioning error the second version of the adaptive approach is proposed. This version is applied to the whole system that is treated as just one area.

Without the partitioning, there is no need in the concept of fictitious generators representing boundary buses of the study area and the external area and the expressions in (1) for the d-axis current and the q-axis current are simplified as:

$$I_{d_i} = \sum_{j=1}^{N_g} E'_{d_j} (G_{ij} \cos \delta_{ij} + B_{ij} \sin \delta_{ij}) + \sum_{j=1}^{N_g} E'_{q_j} (G_{ij} \cos \delta_{ij} - B_{ij} \sin \delta_{ij})$$

$$I_{q_i} = \sum_{j=1}^{N_g} E'_{d_j} (-G_{ij} \cos \delta_{ij} + B_{ij} \sin \delta_{ij}) + \sum_{j=1}^{N_g} E'_{q_j} (G_{ij} \cos \delta_{ij} + B_{ij} \sin \delta_{ij})$$

As the only area of the system contains all generators including the generators from the study area whose dynamics are of the main interests, the transformation and truncation of the states are not performed, and the performance improvement comes only from the linearization of nonlinear functions. In the absence of inputs from the boundary between the study area and the external area, the control matrix  $\mathbf{B}$  is eliminated from (10) and the system used in the second version of the adaptive approach is simplified as:

$$\begin{cases} \dot{\mathbf{x}} = \begin{pmatrix} \hat{\mathbf{f}}(\mathbf{x}, \mathbf{u}) \\ \hat{\mathbf{A}}\Delta\mathbf{x} + \hat{\mathbf{x}}^0 \end{pmatrix} \\ \mathbf{y} = \mathbf{x} \end{cases} \quad (11)$$

where  $\hat{\mathbf{A}} = \hat{P}A$ ;  $\hat{\mathbf{A}} \in R^{(n-q) \times n}$ .

All nonlinear functions representing generators of the study area are contained in  $\hat{\mathbf{f}}$ . The list of linearized functions corresponding to generators of the external area is the same as in the adaptive approach applied to the partitioned system described above. The adaptive switching is performed between systems (11) and (12), i.e. the simplified version of (3).

$$\begin{cases} \Delta\dot{\mathbf{x}} = \mathbf{A}\Delta\mathbf{x} \\ \Delta\mathbf{y} = \mathbf{C}\Delta\mathbf{x} \end{cases} \quad (12)$$

As all generators of the system including those of the study area are linearized in (12) the angle deviation threshold  $\Delta\delta_{\max}$  of the adaptive switching algorithm is set to a small value to enable switches even if oscillations are damped.

### III. CASE STUDIES

Comprehensive case studies are conducted to compare the proposed adaptive model reduction approaches with the traditional linear model reduction approach. A realistic power system model is tested. For the system, the study area is defined and retained with original, detailed models and the rest of the system is defined as the external area to be reduced respectively by different approaches. Then, time-domain contingency simulation using each reduced system model is conducted and compared with the simulation using the original system model. In addition, the approaches are validated during different post-fault operating conditions and compared with the traditional coherency-based model reduction approach.

#### A. Temporary Bus Fault Tests

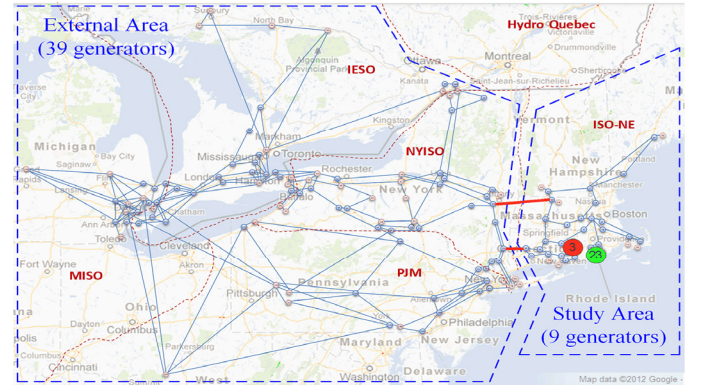


Fig. 3. Partitioned NPCC system.

The linear model reduction approach and the adaptive approaches described above are applied to the NPCC 140-bus 48-generator system shown in Fig. 3. The study area is set to be the ISO-NE region having 9 generators. The external area is set to be the rest of the system, which has 39 generators,  $39 \times 9 = 351$  state variables and  $39 \times 4 = 156$  nonlinear functions since the first 5 state variables of each generator is described by linear differential equations. The external area is connected to the study area by two tie-lines.

The  $H_\infty$  norm of the balanced truncation error is set to be equal to  $10^{-5}$ , corresponding to truncating 200 out of 351 state variables. To find the threshold value of the column norm of the admittance matrix that decides if generator is electrically

close to the boundary, a case study is performed on the system in (10). The threshold decreases with 0.1-p.u. increments from 10 until all rotor angle errors following any of the contingencies are below 6 degrees. After the case study, the threshold is set as 1 p.u. Nonlinear functions corresponding to generators with column norms of the admittance matrix less than 1.0 p.u. are linearized. This corresponds to linearization of 136 out of 156 nonlinear functions of the external area in the case of partitioned system and 136 out of 192 nonlinear functions of the unpartitioned system.

The column norm threshold per unit value is not useful if the proposed approach is applied to a system with a different base power. To make it more practical, it is converted to value in siemens. The NPCC system has the base power of 100 MVA. Setting the base voltage to the common generator terminal voltage of 20 kV the new thresholds is calculated by

$$Y_{th} = 1 \times \frac{S_{base}}{V_{base}^2} = 1 \times \frac{100 \times 10^6}{(20 \times 10^3)^2} = 0.25 S. \quad (13)$$

When the proposed approach is applied to a different system, the threshold is converted to a per unit value using the new system MVA base and the base voltage of 20 kV.

Another case study is performed to select the angle deviation threshold  $\Delta\delta_{max}$  for the adaptive switching algorithm applied to the partitioned system. The threshold is decreased with 1-degree increments from 180 degrees until all rotor angle errors for all generators following any of the contingencies are below 6 degrees. After this case study,  $\Delta\delta_{max}$  is set to 67 degrees. The threshold for the adaptive approach applied to the unpartitioned system is set to 6 degrees to ensure that the rotor angle errors of generators representing study area are also below 6 degrees. The simulations are performed in MATLAB R2015a on the computer with 4-GHz AMD FX-8350 processor and 8 GB of memory. The duration of simulation is set to 16 seconds with an integration time step of 0.01 seconds.

To compare the approach performance during a large disturbance, a three-phase short circuit fault lasting for the critical clearing time (CCT) is created separately at every bus of the study area. CCT is calculated using the original system, CCTs of the adaptively reduced systems are the same as the ones of the original system, CCTs of the linearly reduced system are smaller or equal to the ones of the original system. The errors of all outputs (state variables) of all generators in the study area are analyzed and the rotor angle state variable has the largest error for each of the generators. For every fault, the generator with the largest error of the rotor angle is found and used to compare the approaches. The results of comparison of rotor angle root mean square errors of the linear model reduction and the adaptive approaches are shown in Fig 4. As it can be seen the linear model reduction approach cannot guarantee satisfactory performance during large disturbances generating the errors of more than 25 degrees while the proposed adaptive approach keeps the error for all disturbances within 6 degrees both for the case with the system partitioned into the study and the external area and the case with only one area representing the whole system.

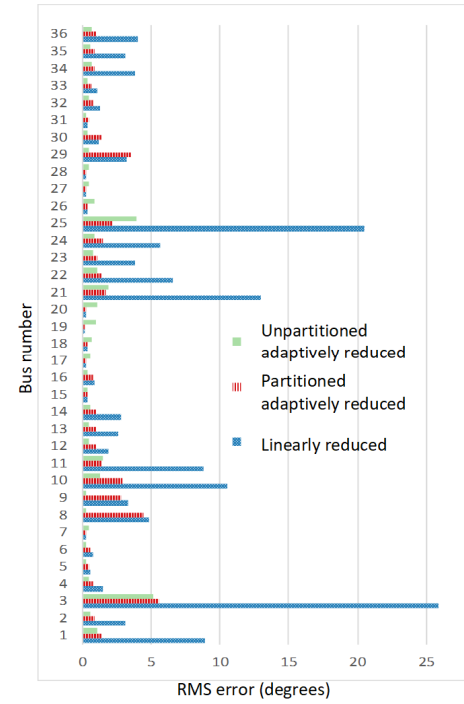


Fig. 4. Comparison of root mean square error of rotor angle.

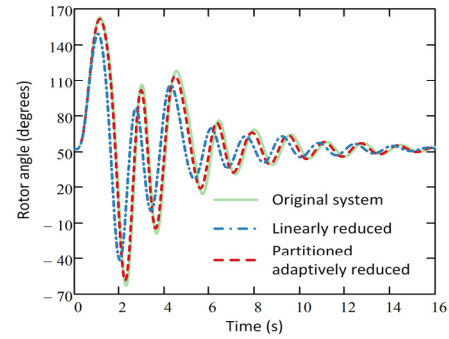


Fig. 5. Rotor angle of generator 23 following the fault at bus 3.

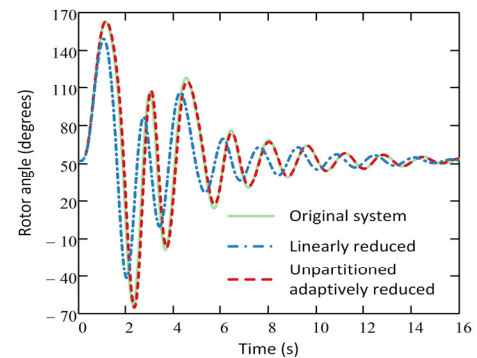


Fig. 6. Rotor angle of generator 23 following the fault at bus 3.

The fault at bus 3 is the largest disturbance of the system and generator 23 has the largest rotor angle error following the fault, and thus its rotor angle is used for the comparison. The simulation results are shown in Fig. 5 and Fig. 6, where the adaptive approach is respectively applied to the partitioned system and unpartitioned system. From the figures, if the external system is reduced using linear model reduction, the rotor angle trajectory differs significantly from that of the original system whereas the rotor angle trajectory of the

system reduced by the adaptive approaches follows accurately the original trajectory.

To present in more detail the difference between approaches, the root mean square errors of all state variables are calculated using the following expression:

$$\varepsilon_i = \sqrt{\sum_{j=1}^N (x_{ij} - \hat{x}_{ij})^2} / N \quad (14)$$

where  $N$  is the number of simulation steps;  $x_{ij}$  and  $\hat{x}_{ij}$  are respectively the values of  $i$ -th state variable of generator 23 of the original system and the reduced system at time step  $j$ . The results of calculation are shown in Table I.

TABLE I

COMPARISON OF ROOT MEAN SQUARE ERROR OF STATES OF GENERATOR 23

States	System models		
	Linearly reduced	Partitioned adaptively reduced	Unpartitioned adaptively reduced
$\delta$ , degrees	$2.24 \times 10^1$	$5.5 \times 10^0$	$5.1 \times 10^0$
$P_m$ , p.u.	$1.8 \times 10^{-3}$	$4.1 \times 10^{-4}$	$3.4 \times 10^{-4}$
$P_{gv}$ , p.u.	$2.3 \times 10^{-2}$	$5.1 \times 10^{-3}$	$4.5 \times 10^{-3}$
$V_R$ , p.u.	$1.7 \times 10^{-1}$	$3.7 \times 10^{-2}$	$4.1 \times 10^{-2}$
$R_f$ , p.u.	$1.3 \times 10^{-2}$	$3.4 \times 10^{-3}$	$3.2 \times 10^{-3}$
$E_{fd}$ , p.u.	$9.8 \times 10^{-2}$	$2.2 \times 10^{-2}$	$2.3 \times 10^{-2}$
$E'_d$ , p.u.	$6.9 \times 10^{-2}$	$1.4 \times 10^{-2}$	$1.5 \times 10^{-2}$
$E'_q$ , p.u.	$1.1 \times 10^{-2}$	$2.8 \times 10^{-3}$	$2.6 \times 10^{-3}$
$\omega$ , p.u.	$4.7 \times 10^{-3}$	$1.0 \times 10^{-3}$	$9.7 \times 10^{-4}$

The proposed adaptive approaches reduce the error by 74% to 81% for every state variable compared to the linear model reduction approach. A fault with the duration equal to CCT is the worst-case scenario that can cause the largest error. The worst-case errors of the proposed adaptive model reduction approach are small enough to justify its applicability to power system stability studies.

In addition to the accuracy the approaches are compared in terms of simulation time as shown in Table II. In Table II the large disturbance corresponds to the 0.39-second fault at bus 3 and the small disturbance corresponds to the 0.03-second fault at bus 17. The results show that the proposed adaptive approach applied to the partitioned system reduces the simulation time by 57% during the large disturbance and by 59% during the small disturbance compared to the original system. If the adaptive approach is applied to the unpartitioned system, the simulation time is reduced respectively by 73% and 84%. The difference in simulation time between two versions of the adaptive approach is caused by the transformation and partitioning in the partitioned system and by the fact that the whole unpartitioned system is switched to the linearized model which is the fastest model. Especially it is clear in the case of the small disturbance as the switching to the linear model happens earlier.

### B. Test of Operating Condition Change

To test the robustness of the adaptive approach against a change of the operating condition, the temporary fault at bus 3

representing the largest disturbance is changed to a permanent fault cleared by tripping one of the lines connected to the bus or by completely isolating the bus by tripping all lines connected. Following the bus fault, the system operating condition is changed. The results of simulation are shown in Table III, from which the proposed adaptive approach can reduce the system after the change of the operating condition while maintaining the accuracy of simulation.

TABLE II  
COMPARISON OF SIMULATION TIME

Systems	Simulation time (s)	
	Large disturbance	Small disturbance
Original unpartitioned	3.7	
Partitioned and linearly reduced	0.9	
Partitioned and adaptively reduced	1.6	1.5
Unpartitioned and adaptively reduced	1.0	0.6

TABLE III  
COMPARISON OF FAULTS LEADING TO A NEW OPERATING CONDITION

Faults	Rotor angle RMS error (deg.)	
	Partitioned adaptively reduced	Unpartitioned adaptively reduced
Temporary at bus 3	5.51	5.12
At line 3-2 followed by the line trip	5.48	5.09
At line 3-4 followed by the line trip	5.28	4.80
At bus 3 followed by the bus trip	2.74	2.04

### C. Comparison with the Coherency-based Model Reduction

Proposed adaptive approaches are compared to another traditional model reduction approach based on grouping coherent generators following a small disturbance, which follows a conventional industry practice in coherency-based model reduction using commercialized software tools SSAT and DYNRED by Powertech Labs. First, the complete eigenvalue analysis is performed in SSAT. Accordingly, three dominant inter-area modes of oscillations between the study and the external area with the largest participation factors of generators of the study area are selected. The frequencies of the selected modes are 0.71 Hz, 0.72 Hz, and 0.77 Hz. Feed the SSAT result into DYNRED and use a tolerance-based method for generator grouping. Then, 17 groups of coherent generators are identified based on the selected modes. The first group of 9 generators correspond to the study area and the other 16 groups represent generators of the external area. The first group plus neighboring 36 buses are set to be the study area. Model reduction by DYNRED aggregates 39 generators of the external area into 16 equivalent generators resulting in a reduced 82-bus 25-generator system.

First, the proposed and traditional approaches are tested using faults at boundary buses. The results of the simulation are shown in Table IV. All approaches provide satisfactory performance. The larger error of the partitioned systems is due to the larger partitioning error during contingencies at the boundary. The largest disturbance (0.39-second fault at bus 3) in the study area makes the coherency-based reduced system unstable. To compare the approaches, the duration of the fault is reduced to 0.38 seconds. The simulation results are shown in Table V. Both traditional linear and coherency-based

approaches provide similar performance in terms of accuracy and speed; however the accuracy of proposed approaches is substantially higher.

TABLE IV

COMPARISON OF MODEL REDUCTION APPROACHES WITH BOUNDARY FAULTS

System	RMS error, degrees	
	Bus 29 fault	Bus 35 fault
Coherency-based reduced	0.93	2.27
Partitioned and linearly reduced	3.15	3.14
Partitioned and adaptively reduced	3.48	0.82
Unpartitioned and adaptively reduced	0.43	0.52

TABLE V

COMPARISON OF MODEL REDUCTION APPROACHES DURING BUS 3 FAULT

System	RMS error, degrees	Simulation time, seconds
Coherency-based reduced	16.98	1.1
Partitioned and linearly reduced	14.14	0.9
Partitioned and adaptively reduced	2.30	1.6
Unpartitioned and adaptively reduced	1.96	1.0

#### IV. CONCLUSIONS

This paper has proposed two versions of a new adaptive model reduction approach that can be applied to traditional partitioned system or to unpartitioned system for fast power system simulation. The approach is capable of accurate representation of the original power system model with significant reduction in computational time.

#### V. REFERENCES

- [1] J. H. Chow, *Power system coherency and model reduction*. Springer, 2013, pp. 1-3.
- [2] J. H. Chow, et al, "Inertial and slow coherency aggregation algorithms for power system dynamic model reduction," *IEEE Trans. Power Systems*, vol. 10, no. 2, pp. 680–685, May 1995.
- [3] R. J. Galarza, et al, "Aggregation of exciter models for constructing power system dynamic equivalents," *IEEE Trans. Power Systems*, vol. 13, no. 3, pp. 782–788, Aug. 1998.
- [4] F. Ma, V. Vittal, "Right-sized power system dynamic equivalents for power system operation," *IEEE Trans. Power Systems*, vol. 26, no. 4, pp. 1998–2005, Nov. 2011.
- [5] B. C. Moore, "Principal component analysis in linear systems: Controllability, observability and model reduction," *IEEE Trans. Automatic Control*, vol. 26, no. 1, pp. 17–32, Feb. 1981.
- [6] S. Liu, "Dynamic-data driven real-time identification for electric power systems," Ph.D. dissertation, Univ. of Illinois at Urbana-Champaign, Urbana, IL, 2009.
- [7] C. Sturk, L. Vanfretti, Y. Chompoobutrgool, H. Sandberg, "Coherency-independent structured model reduction of power systems," *IEEE Trans. on Power Systems*, vol. 29, no. 5, pp. 2418–2426, Sep. 2014.
- [8] L. T. Pillage, R. A. Rohrer, "Asymptotic waveform evaluation for timing analysis," *IEEE Trans. on Computer-Aided Design of Integrated Circuits and Systems*, vol. 9, no. 4, pp. 352–366, Apr. 1990.
- [9] E. J. Grimme, "Krylov projection methods for model reduction," Ph.D. dissertation, Univ. of Illinois at Urbana-Champaign, Urbana, IL, 1997.
- [10] D. Chaniotis, "Krylov subspace methods in power system studies," Ph.D. dissertation, Univ. of Illinois at Urbana-Champaign, Urbana, IL, 2001.
- [11] J. Hahn, T. F. Edgar, "An improved method for nonlinear model reduction using balancing of empirical Gramians," *Computers and Chemical Engineering*, vol. 26, no. 10, pp. 1379–1397, Oct. 2002.
- [12] J. Qi, J. Wang, H. Liu, A. D. Dimitrovsky, "Nonlinear model reduction in power systems by balancing of empirical controllability and observability covariances," *IEEE Trans. on Power Systems*, in press.

- [13] K. Fujimoto, J. M. A. Scherpen, "Singular value analysis and balanced realizations for nonlinear systems," in *Model Order Reduction: Theory, Research Aspects and Applications*, Springer, 2008, pp. 251–272.
- [14] E. I. Verriest, "Time variant balancing and nonlinear balanced realizations," in *Model Order Reduction: Theory, Research Aspects and Applications*, Springer, 2008, pp. 213–250.
- [15] M. Rathinam, L. R. Petzold, "A new look at proper orthogonal decomposition," *SIAM Journal on Numerical Analysis*, vol. 41, no. 5, pp. 1893–1925, 2003.
- [16] M. Striebel, J. Rommes, "Model order reduction of nonlinear systems in circuit simulation: status and applications," in *Model Reduction for Circuit Simulation*, Springer, 2011, pp. 289–301.
- [17] S. Wang, et al, "Dynamic-feature extraction, attribution, and reconstruction (DEAR) method for power system model reduction," *IEEE Trans. Power Syst.*, vol. 29, no. 5, pp. 2049–2059, Sep. 2014.
- [18] P. W. Sauer, M. A. Pai, *Power System Dynamics and Stability*. Englewood Cliffs, NJ: Prentice Hall, 1998, pp. 183-188.
- [19] A. A. Desrochers, R. Y. Al-Jaar, "A method for high order linear system reduction and nonlinear system simplification," *Automatica*, vol. 21, no. 1, pp. 93–100, Jan. 1985.
- [20] X. Ma, J. A. De Abreu-Garcia, "On the computation of reduced order models of nonlinear systems using balancing technique," in *Proc. Decision and Control*, 1988, pp. 1165–1166.
- [21] A. Verhoeven, J. ter Maten, M. Striebel, R. Mattheij, "Model order reduction for nonlinear IC models," in *System Modeling and Optimization*, Springer, 2007, pp. 476–491.
- [22] M. Striebel, J. Rommes, "Model order reduction of nonlinear systems: status, open issues, and applications," Chemnitz University of Technology, Chemnitz, Germany, CSC/08-07, Nov. 2008.

#### VI. BIOGRAPHIES



**Denis Osipov** (S'14) received his B.S. and M.S. degrees in electrical engineering from Donetsk National Technical University, Donetsk, Ukraine in 2004 and 2005 respectively. He is currently pursuing Ph.D. degree in electrical engineering at the Department of Electrical Engineering and Computer Science, University of Tennessee, Knoxville, TN, USA. His research interests include power system voltage stability, power system model reduction and high-performance computing.



**Kai Sun** (M'06–SM'13) received the B.S. degree in automation in 1999 and the Ph.D. degree in control science and engineering in 2004 both from Tsinghua University, Beijing, China. He is currently an associate professor at the Department of EECs, University of Tennessee, Knoxville, TN, USA. He was a project manager in grid operations and planning at the EPRI, Palo Alto, CA from 2007 to 2012. Dr. Sun serves in the editorial boards of IEEE Transactions on Smart Grid, IEEE Access and IET Generation, Transmission and Distribution. His research interests include stability, dynamics and control of power grids and other complex systems.